32nd EPS Conference on Plasma Phys. Tarragona, 27 June - 1 July 2005 ECA Vol.**29C**, O-4.002 (2005)

Nonlinear Dynamics and Energy Loss Mechanisms of ELMs

P.B. Snyder[1], H.R. Wilson[2], X.Q. Xu[3]

[1]*General Atomics, P.O. Box 85608, San Diego, California 92186-5608, USA*
[2]*Culham Science Centre, Oxfordshire, UK*
[3]*Lawrence Livermore National Laboratory, Livermore, USA*

The peeling-ballooning model [1,2] proposes intermediate wavelength MHD modes driven by the pressure gradient and current in the pedestal region as a mechanism for edge localized modes (ELMs) and constraints on the H-Mode pedestal in tokamaks. The model has successfully explained onset conditions and a number of observed characteristics of many types of ELMs [e.g. 2-4]. An important tool for the development of the peeling-ballooning model is the ELITE [2,5] MHD stability code. A growth rate spectrum (n=4-1000) calculated for a D-shaped equilibrium by ELITE is given in Fig 1(a), along with low and high n benchmarks. Figure 1(b) shows a typical (n=18) mode structure of a peeling-ballooning mode in the DIII-D tokamak.

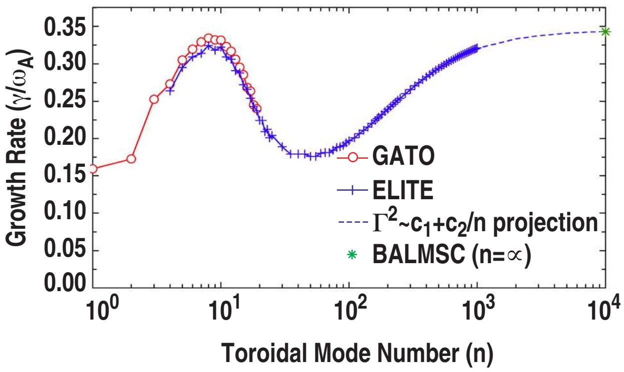

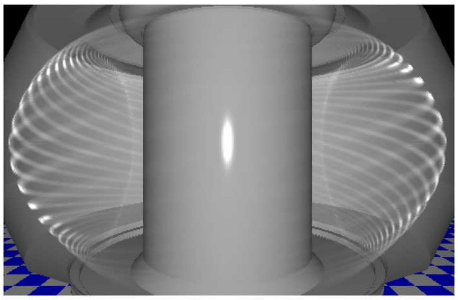

Fig. 1. (a) Growth rate spectrum with benchmarks, and (b) 3D rendering of mode structure of an edge localized peeling-ballooning mode.

Recent studies have incorporated toroidal flow shear into ELITE, leading to significant effects on growth rate and mode structure, and implications for ELM dynamics. Fig. 2(a) shows growth rates as a function of toroidal rotation shear for various mode numbers. A rotation shear value of ~50-100 kHz in the units shown is typical of the H-mode edge in existing experiments such as DIII-D. High n modes are strongly suppressed, in agreement with infinite-n theory. However, the growth rate and stability threshold of the lower range of peeling-ballooning modes (n~3-20) is relatively weakly affected, though the mode structure of these instabilities changes significantly. Typically modes are narrowed in the radial direction, sometimes with a change of phase in the radial displacement near the middle of the pedestal. Because these modes have a single eigenfrequency, they can match the sheared rotation frequency (nΩ) of the plasma at only one radial location, typically

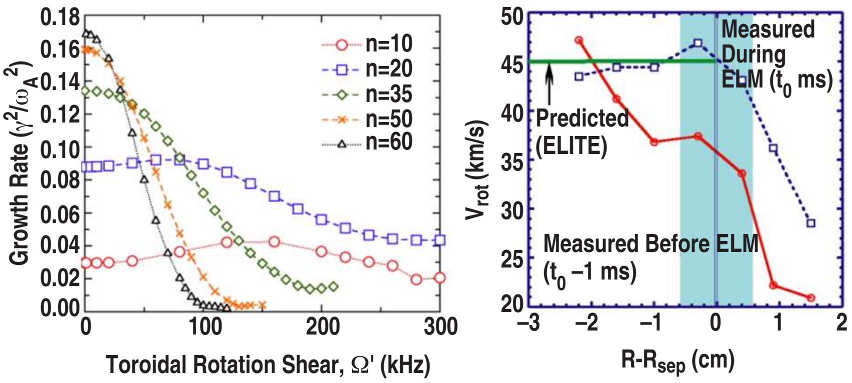

Fig. 2. Growth rate vs toroidal flow shear for various n. (b) Measured rotation before and during an ELM compared with ELITE calculation of the eigenfrequency of the most unstable mode.

near the middle of the mode structure. We have taken the measured density, temperature and toroidal rotation profiles from a DIII-D discharge shortly before an ELM is observed, and calculated the most unstable mode number (n=9) and its eigenfrequency. That eigenfrequency is then compared to the measured rotation profile during an ELM in Fig. 2(b). The agreement between the calculated mode eigenfrequency and the observed plasma rotation during the ELM suggests that mode growth strongly damps sheared flow in the edge. The sheared toroidal flow is a primary component of the ExB shear which is thought to create the edge transport barrier. Hence, the collapse of the sheared rotation is posited to result in a collapse of the edge transport barrier during the ELM.

While linear stability studies have proved useful for understanding ELM onset and pedestal constraints, quantitative prediction of ELM size and heat deposition on material surfaces requires nonlinear dynamics. Here we focus on the scales of the fast ELM crash event itself, initializing simulations with peeling-ballooning unstable equilibria and following the mode dynamics into the strongly nonlinear phase. We employ the 3D reduced Braginskii BOUT code [6,7], modified to include the equilibrium kink/peeling drive term [7]. BOUT employs field-line-following coordinates for efficiency, and simulates the pedestal and SOL regions (typically $0.9 < \Psi_N < 1.10$, where Ψ_N is the normalized poloidal flux). We study a set of high density DIII-D H-mode discharges. An example is shown in Fig. 3. Figure 3(a) shows the mode growing up linearly in the sharp gradient region of the pedestal at early times, and then at later times (t>~2000) a very rapid burst occurs resulting in the expulsion of particles and heat across the separatrix in a filamentary structure that is radially extended but localized in the cross field direction, as shown in Fig. 3(b). In the linear phase, the mode has the expected peeling-ballooning structure [similar to Fig. 1(b)], while at late times the formation of either one [Fig. 3(b)] or several [Fig. 4(c)] radially propagating filaments is possible, depending on initial conditions and flatness of the mode spectrum. The explosive growth observed at late times has been studied [8] and found to be qualitatively similar to expectations from nonlinear ballooning theory [9].

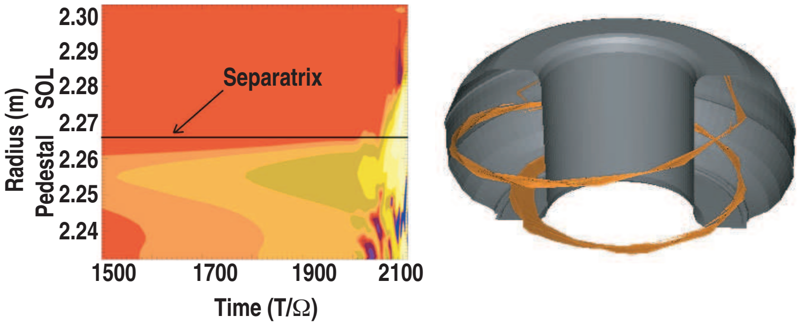

Fig. 3. (a) Contour plot of the evolution of the perturbed density on the outboard midplane. (b) Surface of constant perturbed density at t=2106 shows radially propagating filamentary structure.

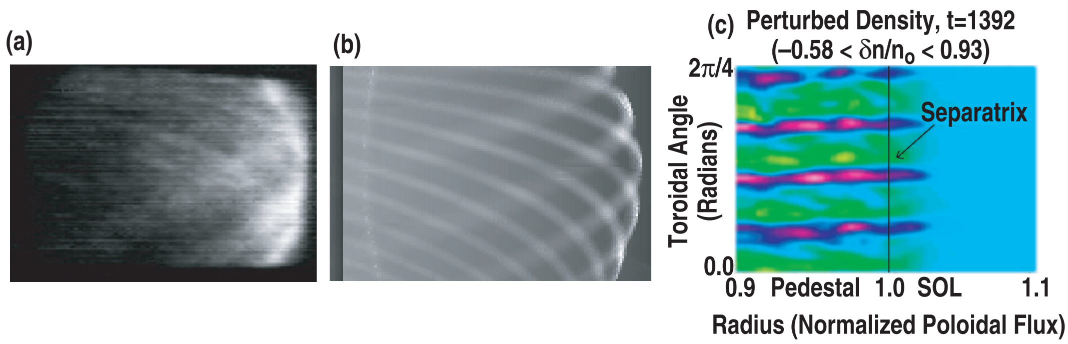

Fig. 4. (a) CIII image during an ELM event in DIII-D, (b) calculated ELITE mode structure (n=18) viewed from approximately the CIII camera's viewing angle. (c) Nonlinear BOUT simulation shows the filaments breaking up and propagating radially across the separatrix.

Filamentary structures, qualitatively similar to those found in the simulations, have been observed during ELMs on multiple tokamaks. Recent observations [10] of CIII emission during the ELM event on the DIII-D tokamak similarly show a filamentary structure, as shown in Fig. 4(a). Estimates based on the spacing between filaments suggest a mode number of approximately n~18. For this case, an equilibrium has been reconstructed using profiles measured shortly before the observed ELM. Using ELITE, this equilibrium is found to be marginally unstable, with the most unstable mode number falling in the range $15 < n < 25$. The mode structure calculated by ELITE for $n = 18$ has been rendered in 3D, and is shown in Fig. 1(b). A view of this mode structure similar to the fast camera view is shown in Fig. 4(b). Note that both the apparently broad (because of proximity to the camera) filaments in the near field and the apparently narrow filaments in the far field of the camera are qualitatively similar between the observation and the calculated linear mode. The observations are expected to correspond to the nonlinear phase of the ELM. Nonlinear simulations with BOUT have also been carried out for this case. In the early phase of these simulations, the mode structure is symmetric and similar to the linear structure shown in Fig. 4(b). During the explosive nonlinear phase the mode develops a degree of asymmetry as shown in Fig 4(c), with 4 filaments propagating outward in a 1/4 toroidal domain (16 filaments total).

We note that these filamentary structures observed in the simulations and in experiment are associated with the ELM event, but because of their relatively small volume, direct loss of the energy and particle content of the one (or many) filaments alone cannot account for the large losses of energy and particles in the full ELM crash. We propose two mechanisms to explain these losses. In the first mechanism, the filaments act as conduits, which remain connected to the hot core plasma. Fast diffusion and/or secondary instabilities in the outward propagating region of the filament allows loss of particles and heat from the filament to nearby open field line plasma. The ends of the field line remain connected to the hot core plasma, allowing parallel flow and consequent loss of a substantial amount of heat and/or particles from the core. In the second mechanism, the growth and propagation of the filament causes a collapse of the edge rotation shear and hence the edge transport barrier, resulting in a temporary return of L-mode-like edge transport, and rapid loss of particles and heat from the edge region. We propose these two mechanisms together to explain observed ELM losses, and note that the observed decrease in energy losses at high collisionality is consistent with the expected reduction in losses via the "conduit" mechanism.

This work was supported by the U.S. Department of Energy under De-FG03-95ER54309, the UK Engineering and Physical Sciences Research Council, and Euratom. Contributions by D.P. Brennan, S. Cowley, M.E. Fenstermacher, W. Meyer, M. Umansky, M.R. Wade, and the DIII-D Team.

[1] J.W. Connor, R.J. Hastie, H.R. Wilson *et al*, Phys. Plasmas **5**, 2687 (1998).
[2] P.B. Snyder, J.R. Wilson, J.R. Ferron, *et al.,* Phys. Plasmas **9**, 2037 (2002).
[3] P.B. Snyder, H.R. Wilson, J.R. Ferron *et al.,* Nucl. Fusion **44**, 320 (2004).
[4] D.A. Mossessian, P. Snyder, *et al.,* Phys. Plasmas **10**, 1720 (2003).
[5] H.R. Wilson, P.B. Snyder, *et al*, Phys. Plasmas **9**, 1277 (2002).
[6] X.Q. Xu, R.H. Cohen, W.M. Nevins, *et al.,* Nucl. Fusion **42**, 21 (2002).
[7] X.Q. Xu, W.M Nevins, *et al.,* New J. Physics **4**, 53 (2002).
[8] P.B. Snyder, H.R. Wilson, and X.Q. Xu, Phys. Plasmas **12** 056115 (2005).
[9] H.R. Wilson and S.C. Cowley, Phys. Rev. Lett. **92**, 175006 (2004).
[10] M.E. Fenstermacher, A.W. Leonard, *et al.,* submitted to Nucl. Fusion (2004).